Solid-State ^{13}C NMR Study of Thermotropic Poly(bibenzoates). 2. Poly(triethylene glycol *p,p'*-bibenzoate)

Ernesto Pérez, Rosario Benavente, Antonio Bello, and José M. Pereña

Instituto de Ciencia y Tecnología de Polímeros (CSIC), Juan de la Cierva 3, 28006 Madrid, Spain

David L. VanderHart*

Polymers Division, National Institute of Standards and Technology, Gaithersburg, Maryland 20899

Received March 14, 1994; Revised Manuscript Received March 25, 1995[⊗]

ABSTRACT: Several samples of thermotropic poly(triethylene glycol *p,p'*-bibenzoate) (PTEB) with different thermal histories have been analyzed by DSC, X-ray scattering, and solid-state ^{13}C and ^{1}H NMR. This polymer can be quenched into the smectic LC state and becomes semicrystalline (≈0.39 crystalline fraction) upon annealing for 12 days at 85 °C (sample 85A). Also, annealing for 33 months at ambient temperatures (sample RTA1) yields a ≈31%-crystalline sample, owing to a T_g of 20 °C. By ^{13}C NMR, the spectra of the crystalline fraction of these two semicrystalline samples are isolated. These two spectra, in the aromatic region, are very similar; however, in the aliphatic region there are significant differences which probably originate from conformational differences within the spacer. DSC data show a significant contrast in crystalline melting points for the RTA1 and 85A samples. Small-angle synchrotron and NMR spin diffusion data, combined with crystallinity values, yield a picture of relatively thin crystallites, about 3 repeat units thick in the 85A sample and about 2 units thick in the RTA1 sample so there is some question as to whether the crystallites are thick enough to express their undistorted crystalline habit in the isolated NMR spectra and whether the melting point difference can be attributed to different crystal thicknesses, as opposed to polymorphism. Synchrotron data taken in the region of the smectic layer spacing show that layer spacings persist in all samples, quenched or annealed. Yet there are definite changes in these layer spacings which accompany crystallization. In view of the thin nature of the crystallites, however, the relatively narrow width of these synchrotron peaks suggests a periodicity which must encompass both the noncrystalline (NC) and the crystalline regions. Selected NMR relaxation measurements also bear out the notion that molecular mobility within the LC regions of quenched samples and the NC regions of semicrystalline samples is similar, although not identical. Finally, the ^{13}C spectral observations in the region of the aliphatic carbons for the 85A sample suggest one of two possibilities: either the spacer conformation in the interior of the crystallites differs from the conformation near the crystal/NC interface or there is polymorphism. A split peak for the layer line in the synchrotron data also supports the notion of polymorphism.

Introduction

The interest in liquid crystalline (LC) polymers has grown extraordinarily in recent years. Among them, polyesters incorporating mesogenic units into the main chain form an important class of thermotropic polymers[1,2] which usually exhibit a mesophase at temperatures above the region of the crystalline solid and below the onset of the isotropic melt. However, the requirement that the mesogen be a rather rigid structure often leads to high crystal/LC transition temperatures with the result that chemical degradation becomes a problem. The introduction of flexible aliphatic spacers is a widely used method of reducing high transition temperatures. The amount of that reduction depends not only on the length of the spacer but also on the presence of ether linkages.

Several studies have been performed on poly(bibenzoates) showing the ability of the biphenyl group to generate smectic mesophases. For those polymers incorporating all-methylene spacers, a rapid transformation of the LC phase into a three-dimensional crystal structure has been found.[3–8] In contrast, when oxygen atoms are included in the spacers, that transformation is greatly inhibited[7–10] in such a way that the mesophase is stable at room temperature for a considerable time. This is the case of poly(triethylene glycol *p,p'*-bibenzoate) (PTEB). Some aspects of the thermotropic behavior of this polymer have been recently analyzed,[7] including a consideration of the conformational characteristics that can influence the formation and stability of the liquid crystalline phase.

Solid-state ^{13}C NMR is a convenient tool for probing molecular organization in polymeric solids. For spectra observed in the presence of high-power proton decoupling and magic angle spinning (MAS)[11] one can often distinguish resonances arising from ordered crystalline regions from those associated with disordered regions.[12] Contrast in relaxation times for these two regions are also obtained, owing to differences in mobility.[13,14] Moreover, ^{13}C MAS spectra often reveal magnetic inequivalences in the crystalline unit cell for carbons that exhibit single resonances in solution; this provides valuable information for structure determination.[15–16] Crystalline polymorphism, when present, can also be detected.

Our first paper[17] in this series dealt with two closely related bibenzoates; one, poly(heptamethylene *p,p'*-bibenzoate), (P7MB) had a seven-methylene spacer and the other, poly[oxybis(trimethylene) *p,p'*-bibenzoate] (PDTMB) had a similar spacer where the central methylene was replaced by an oxygen atom. PDTMB is similar to PTEB in the sense that a smectic phase lies between the crystalline phase and the isotropic melt; moreover, both can be quenched into the LC phase. For

[⊗] Abstract published in *Advance ACS Abstracts,* August 1, 1995.

0024-9297/95/2228-6211$09.00/0

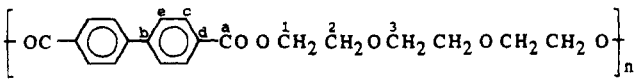

Figure 1. Chemical structure of PTEB with carbon designations.

PDTMB, it was demonstrated from ^{13}C NMR measurements that crystallization modifies the noncrystalline (NC) phase dynamically. It was also observed that the lower angle X-ray peak, which arises from the LC layer spacing in quenched PDTMB, persisted after crystallization, albeit at a slightly shifted position. On the basis of the NMR observations and the slight shift in the X-ray peak position, it was surmised that in the annealed sample this peak arises from the periodicity of the crystalline phase in the chain-axis direction. However, a recent electron microscopy study[18] dealing with another backbone-LC smectic polyester demonstrated that crystallization from the pure LC state can take place while preserving the periodicity of the original smectic phase. Therefore, one objective of this study is to inquire into the similarity between the NMR characteristics of the LC and annealed-NC phase.

PTEB also exhibits DSC behavior which raises questions about multiple crystalline forms. Therefore, we will also investigate the possibility of polymorphism.

This study utilizes the techniques of DSC, X-ray scattering and solid-state ^{13}C and proton NMR to compare PTEB in its quenched, LC state with PTEB in two annealed, semicrystalline states.

Experimental Section

PTEB was synthesized by melt transesterification of diethyl *p,p'*-bibenzoate and triethylene glycol, using isopropyl titanate as catalyst. The details of the preparation and characterization of the sample have been given elsewhere.[7] The chemical structure of PTEB is shown in Figure 1. The value of the intrinsic viscosity, measured at 25 °C in tetrachloroethane, is 1.15 dL g^{-1}.

A film of PTEB was prepared by melting in a Collin press at 150 °C for 5 min, followed by cooling to room temperature. Part of the sample was annealed in a thermostatic bath at 85 °C for 12 days and was subsequently stored at room temperature for more than 1 year prior to its analysis (sample 85A). Another part of the sample was subsequently quenched from the melt (150 °C) and immediately analyzed (sample Q) by different techniques. A portion of this latter sample was held in the laboratory at ambient temperature (22–25 °C) for 33 months (sample RTA1) and then analyzed by ^{13}C NMR. A parallel, but different sample, Sample RTA2, also originally quenched, was held at room temperature for about 12 months and then analyzed by DSC and X-ray methods.

^{13}C spectra were taken at ambient temperature on a noncommercial spectrometer operating at 25.193 MHz (2.35 T). The probe incorporates a 7 mm rotor/stator combination made by Doty Scientific.[19] MAS frequencies were typically 3.5 kHz, and the nutation frequencies associated with the ^{13}C and proton rf fields were 69 and 66 kHz, respectively. Cross polarization (CP) times were 1 ms unless otherwise noted.

Proton spectra were acquired at 200.05 MHz on a CXP200 Bruker spectrometer. T_{1xz} relaxation[20] utilized MREV-8[21,22] multiple pulse irradiation with 90° pulse widths of 1.5 μs, cycle times of 38.4 μs, and a total irradiation time of 39 ms. (The fact that T_{1xz} relaxation takes place under multiple pulse irradiation means that spin diffusion is quenched during this relaxation; T_{1xz} is very similar to the proton rotating frame relaxation, $T_{1\rho}^{H}$, in its sensitivity to molecular motion.[23]) The details of the related T_{1xz}–spin-diffusion measurement, which was used to corroborate the long period obtained from the synchrotron data, have been previously described.[24] The concept of the T_{1xz}–spin-diffusion experiment, as we will use it, is that T_{1xz} for protons in crystalline regions is long; it is shorter for NC protons. Thus, in the first stage of the experiment, one lets T_{1xz} relaxation proceed for a time long enough (34.6 ms) to strongly attenuate proton polarization in the NC regions while preserving a significant fraction of the initial polarization in the crystalline regions. Then, one stores this polarization along the static field. Following this, there is a variable time, t_{sd}, during which spin diffusion is allowed to occur. The last stage of the experiment is the observation of the T_{1xz} decay. At short t_{sd} values, this decay is dominated by the protons in the crystalline regions; owing to spin diffusion, the decay progresses back to an "equilibrium" shape where contributions from all regions are equally represented. As will be seen, the time required for restoring equilibrium can be interpreted in terms of the distance between crystallites. Static samples were employed since our experience is that spinning samples can develop spurious relaxation so as to destroy the correlation between molecular mobility and the time constants obtained from the T_{1xz} experiment.

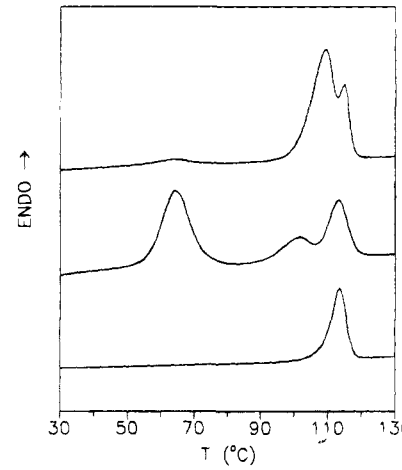

Figure 2. DSC melting curves for the various PTEB samples: Q (lower), RTA2 (middle), and 85A (upper).

The thermal transitions were determined with a Perkin-Elmer DSC7 calorimeter at a rate of 20 °C min^{-1}.

X-ray diffractograms at wide angles (WAXD) were obtained with an X-ray diffractometer from Philips Co. equipped with a Geiger counter detector, using nickel-filtered Cu Kα radiation.

Small- and intermediate-angle X-ray experiments were obtained at Daresbury Laboratory, U.K. (station 8.2) using synchrotron radiation. Rat tail collagen (L = 67.0 nm) was used for calibration. The sample–detector distance was 1.6 m, covering the spacings range from about 1.4 to 40 nm.

Some details of the structural characterization of these samples, together with a dynamic mechanical analysis, have been previously reported.[25]

Results and Discussion

Thermal Analysis. The melting patterns of the three samples of PTEB are presented in Figure 2. Only one transition, corresponding to the isotropization of the mesophase,[7] is found for sample Q with a peak temperature of 114 °C. In contrast, several endotherms are observed for sample 85A: a small one around 64 °C, the largest peak at 108 °C, and a final endotherm, partially overlapped with the previous one, at 114 °C. Sample RTA2 has a dominant endotherm at 64 °C and secondary peaks at 101 and 113 °C. In the interpretation of these DSC data, we assign the 113–114 °C peaks to the isotropization of the mesophase. The peaks at 101–108 °C are assigned to the melting of a crystalline phase. The peak at 64 °C is also tentatively assigned to the melting of a crystalline phase. The multiple endotherms at lower temperatures exhibited by the annealed samples raise the question of crystalline polymorphism. Other possible origins for such multiple

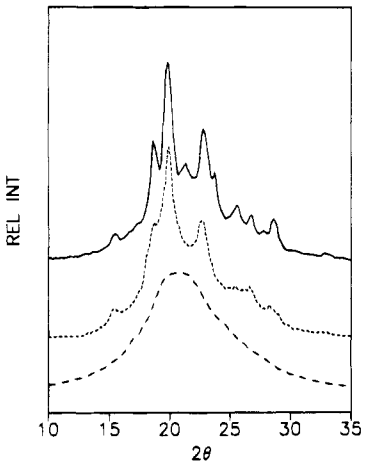

Figure 3. Ambient-temperature X-ray diffractograms of PTEB samples: 85A (—), RTA2 (- - -), and Q (— — —). For clarity, experimental noise, whose rms amplitude is less than 2% of the diffractogram maxima, has been removed by retracing.

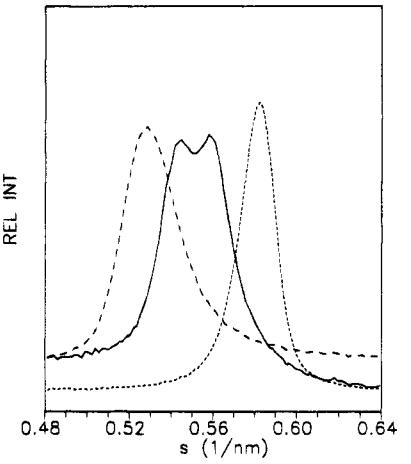

Figure 4. Intermediate-angle synchrotron profiles as a function of the scattering vector, s, for PTEB samples: Q (— — —), RTA2 (- - -), and 85A (—).

endotherms include another LC phase or melting determined by finite crystal size. Note also that the glass transition temperature of PTEB is about 20 °C;[7,10,25] hence, annealing can proceed at room temperature.

X-ray and Synchrotron Results. Previously reported WAXD photographs[7] of a PTEB-Q sample have established the existence of a sharp diffraction (and its second-order peak) corresponding to the LC layer spacing of 1.85 nm. In that same work, a PTEB-Q sample was stretched and from its WAXD pattern it was deduced that PTEB produces a smectic-C mesophase, where the chain direction is tilted by about 23° with respect to the layer-plane normal. The implied chain length is 2.01 nm, which is considerably smaller than the 2.21 nm calculated for the PTEB monomeric unit in extended conformation.

The WAXD patterns, not including the layer line, of the three specimens of PTEB can be observed in Figure 3. The diffractogram corresponding to the Q sample shows only an amorphous-like halo centered near 0.43 nm. The top diagram in Figure 3 corresponds to the 85A sample. Several sharp diffraction peaks, characteristic of three-dimensional order, can be observed. The middle diffractogram in Figure 3 corresponds to sample RTA2, where several diffraction peaks are also observed; yet peaks are fewer and have less resolution than those for sample 85A. Most peaks in the RTA2 diffractogram have counterparts in the 85A diagram; however, the peak near $2\theta = 23°$ shows a slight relative shift. If the main, broad diffractogram peak of the Q sample is taken to be a representation of the NC region of the annealed sample, then one can estimate that the crystallinity of the 85A sample is 0.45 ± 0.05, while a value of 0.40 ± 0.05 is obtained for sample RTA2. Note that in other LC bibenzoates, the main, broad diffractogram peak is very similar for the LC and the molten states,[6,9] so the foregoing assumption should be reasonable.

The Q, RTA2, and 85A PTEB samples have also been analyzed by SAXD at room temperature in a synchrotron source. The corresponding profiles in the region of spacings around 1.8 nm (scattering vector, s, about 0.55 nm^{-1}) are shown in Figure 4. The Q sample exhibits a peak centered at 1.893 ± 0.005 nm. The RTA2 sample shows a single peak at 1.723 ± 0.005 nm whose half-width is only about 65% that of the quenched sample. This peak could represent either persistent LC character in the NC regions of this sample or the repeat distance along the chain axis for the crystalline phase or a combination of both if the periodicities of both phases lie close to one another. In contrast, the profile of the 85A sample (continuous line) is split into two peaks, centered at 1.85 ± 0.01 and 1.78 ± 0.01 nm. Again the organization within the domains giving rise to these separate peaks is not well understood, although one possibility invokes crystalline polymorphism. Nevertheless, if we consider possible polymorphism, there is a qualitative conflict with the DSC data just presented because the DSC trace for the 85A sample indicates a dominance of the material whose endotherm appears at 108 °C, while the synchrotron data suggest that there are comparable volume fractions to be assigned to each peak.

The appearance, in semicrystalline samples, of a smaller angle diffraction peak very close to that characterizing the smectic-LC layer spacing seems to be general in poly(bibenzoates).[6,17] The shift in peak position upon crystallization is often so small that resolution at the synchrotron level is needed. While we had previously argued[17] that for semicrystalline PDT-MB this peak arises from the crystalline domains, the electron microscopy study mentioned earlier[18] on a polyester smectic LC having a bulkier mesogen showed that it is possible to have crystallization and simultaneously maintain the approximate registry of the LC layers. If this is a general result, then the synchrotron peak position may be determined by a combined periodicity including both the crystalline domains and the LC (NC) domains. Thus, it seems reasonable that the synchrotron peak in semicrystalline samples is influenced by the persistence of periodicity in the NC regions. By implication, then, the appearance of shifted or multiple peaks in Figure 4 is not direct, but only indirect, evidence of polymorphism.

Average morphological repeat distances in a semicrystalline sample may be obtained from the small-angle scattering region of the synchrotron data. These data are shown in Figure 5. The Q specimen does not exhibit any defined long spacing (up to the experimental limit of 40 nm), supporting the idea of large coherence lengths in the liquid-crystalline state. The 85A sample, however, presents a very evident long spacing, centered about 13.8 nm. Considering the X-ray crystallinity of the sample and assuming a simple two-phase lamellar model, the estimated crystal thickness is rather small,

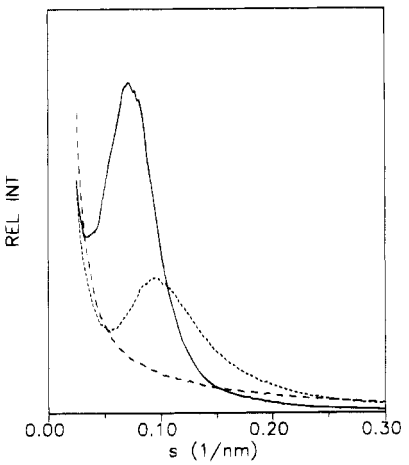

Figure 5. Small-angle synchrotron profiles as a function of the scattering vector, s, for PTEB samples: Q (– – –), RTA2 (- - -), and 85A (—).

i.e., only about 3–4 monomeric units. For the RTA2 sample, the average long spacing is about 10.6 nm and the average crystal is thick enough to incorporate only about 2 repeat units. Thus, the crystal thicknesses of both annealed samples is small. Moreover, returning to the interpretation of the synchrotron peak associated with layer spacing, one would not expect that these relatively narrow peaks could arise solely from the periodicity of such thin crystallites; periodicity in the NC region seems mandated.

NMR Results. 1. Perspective. The NMR results we choose to discuss should be put in the following perspective. The ^{13}C spectrum of the crystalline regions will be isolated; this isolation will pertain to issues of polymorphism as well as crystalline fractions. In addition, we seek further support for the morphology deduced from the synchrotron and X-ray data. This data suggested the existence of both thin crystallites and rather narrow layer lines. In turn, the latter imply a periodicity of layering which includes both the crystalline and NC regions; i.e., the organization of the NC regions is similar to that of the LC. In support of this picture, NMR data will be used to establish the following points: First, T_{1xz}–spin-diffusion results will offer a second estimate of the "long spacing", the mean distance between crystallites. This will verify the deduction about thin crystallites by eliminating any possibility that the small-angle peak in the synchrotron data is associated with a periodicity shorter than the overall periodicity. These diffusion results will also be sensitive to the possibility that large domains of LC organization still remain and are responsible for the synchrotron layer lines. Secondly, if the NC region has a layered structure similar to the LC organization, then one would expect the chain dynamics in both of these regions to be similar, although not necessarily identical, since chain motion is somewhat constrained by periodic confinement in a crystalline region. Since relaxation times are monitors of molecular motion, we, therefore, compare certain relaxation times associated with these regions with the modest goal of showing only similarity.

2. Extent of Motional Averaging. One-pulse, proton Bloch decay spectra of all of the samples showed the absence of any narrow spectral features associated with near-liquid-like mobility. The Q sample had a roughly Gaussian line shape with a full width at half-height of 25 kHz. Line widths for the RTA1 and 85A samples were 28 and 29 kHz, respectively; moreover,

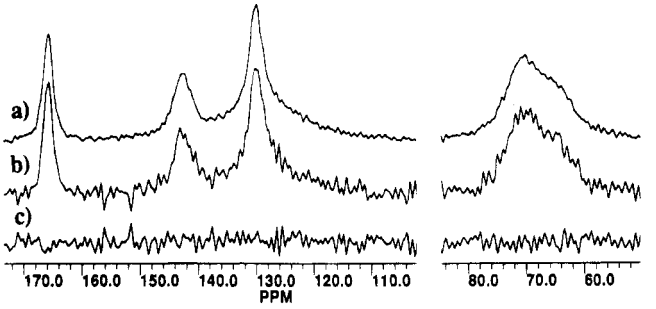

Figure 6. 25 MHz ^{13}C CPMAS spectra of quenched PTEB: (a) SL time = 1 μs, (b) SL time = 2.3 ms; (c) = (a) – (b). Vertical scaling of (b) is chosen for line shape comparison.

these lines were broader at their base than for the Q sample, ostensibly since the aliphatic spacers show some motional averaging in the Q sample and some fraction of these become rigid in the other samples. The absence of any evident spectral components with line widths below 10 kHz implies that any motional averaging taking place has considerable anisotropic character; i.e., unaveraged intramolecular dipolar interactions are not small relative to their rigid-molecule values. This, in turn, means that we do not have to be concerned that certain ^{13}C nuclei will have very sluggish cross-polarization rates as a result of near-isotropic motions. This qualitative inference about the anisotropy of motion is entirely consistent with constraints on any aliphatic spacer bridging mesogens located in the separated layers of a LC.

3. Isolation of ^{13}C Spectra of Crystalline Regions. The ^{13}C CPMAS spectra of the Q sample acquired with variable proton spin locking (SL) times of 1 μs and 2.3 ms prior to cross polarization (CP) are shown in Figure 6a and 6b, respectively. These line shapes do not change with the SL time (the difference spectrum, Figure 6c, is featureless), indicating that $T_{1\varrho}^{H}$ is quite uniform throughout the sample over a distance scales of 3–4 nm. (Potential polarization gradients arising from heterogeneities of $T_{1\varrho}^{H}$ within that range will largely dissipate over 2.3 ms as a result of spin diffusion in the rotating frame.) The most probable interpretation of this uniform $T_{1\varrho}^{H}$ is that a single phase is present, namely, the mesophase. This is also consistent with the thermal and diffraction data. Spectra (not shown) taken with a shorter CP time did not reveal any additional spectral components with short $T_{1\varrho}^{H}$'s. From the data of Figure 6 we deduce a $T_{1\varrho}^{H}$ of 2.3 ms.

The resolution apparent in Figure 6 is quite poor; hence, this sample probably contains significant dynamic and/or positional disorder. The correspondence between the solution-state chemical shifts and those of the solid is reasonable as Table 1 indicates. (Table 1 includes spectral assignments.) By inspection of these spectra, we might be alerted to the following possibilities: First, the relatively symmetric broad features centered around 128 ppm probably indicate that the protonated aromatic carbons possess an "uncertainty-type" broadening; most likely this arises from a substantial spectral density of motion in the mid-kilohertz range.[26] Second, the aliphatic carbon resonance (60–75 ppm), by virtue of its asymmetry, is more likely to have a line shape dominated by a dispersion of chemical shifts rather than molecular motion. Proof of the above statements is offered later in connection with relaxation measurements.

In Figure 7, spectra of the RTA1 sample are shown. Spectra 7a and 7b, respectively, correspond to SL times

Table 1. ^{13}C Chemical Shifts[a] of the Various PTEB Samples Compared to Those in Solution

	CR component		NC component			
carbon[b]	85A	RTA1	85A	RTA1	Q	solution[c]
a	165.3	165.3	166	165.8	165.8	166.2
b	140.2	140.3	142[d]	142[d]	142.5	144.3
c,d	131.9	131.9	130.4	130.3	130.0	130.3 (=c)
		130.5				129.6 (=d)
e	125.2	125.3	125[d]	???[d]	???[d]	127.2
1,2,3	71.1	71.0	70[d]	70[d]	70[d]	70.7 (=3)
	69.7	69.7	64[d]	64[d]	64[d]	69.3 (=2)
	67.9	67.7				64.2 (=1)
	64.6[d]					
	63.4[d]					

[a] Uncertainty in chemical shift values is ±0.3 ppm unless otherwise indicated. [b] See Figure 1 for assignments. [c] In solution of deuterated chloroform (ref 7). [d] Imprecisely defined owing to partial resolution or broad resonances.

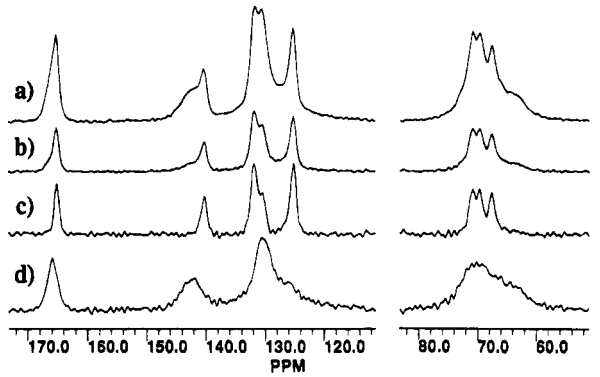

Figure 7. ^{13}C CPMAS spectra of the RTA1 sample: (a) SL time = 1 μs; (b) SL time = 5 ms. Remaining spectra are linear combinations of (a) and (b) chosen to correspond to the crystalline, (c), and NC, (d), components. Criteria for isolating (c) and (d) are discussed in the text. Vertical scaling of (a) and (b) is constant and represents true signal strength as a function of SL time; vertical scaling for c) and d) is chosen so that their sum approximates spectrum a.

of 1 μs and 5 ms. By taking linear combinations of these spectra,[27] one can deduce the line shapes for the crystalline (Figure 7c) and NC (Figure 7d) components. Vertical scaling for these latter two is chosen so that their sum approximates spectrum 7a. The criteria used in determining each line shape is that the "crystal" spectrum is that linear combination which most enhances the sharper spectral features and excludes the formation of any regions of negative intensity. The criteria for generating the NC spectrum are that one enhances the broadest features while suppressing negative intensity in the regions of the "crystal" resonances. Owing to the characteristic that narrower "crystal" resonances are generally superposed on (as opposed to isolated from) the broader NC resonances, there is more uncertainty in the isolation of the NC, relative to the "crystal", lineshape. Nevertheless, from this kind of analysis, one can obtain the apparent crystallinity associated with spectrum 7a; it is 0.32 ± 0.04.

Figure 8 shows spectra for the 85A sample in a format parallel to Figure 7. Spectra 8a–8d respectively correspond to the experimental spectra having SL times of 1 μs and 7 ms, followed by the linear combination spectra for the "crystal" and NC components. The apparent crystallinity in spectrum 8a, according to this analysis, is 0.45 ± 0.04.

4. Crystallinity. We obtain crystallinity estimates from both proton and ^{13}C results. Unfortunately, the

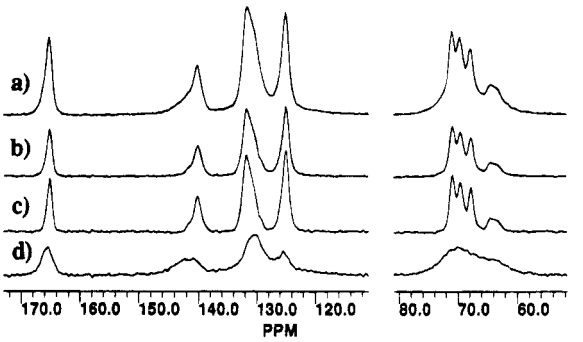

Figure 8. ^{13}C CPMAS spectra of the 85A sample in the same format as Figure 7: (a) SL time = 1 μs, (b) SL time = 7 ms, (c) "crystal" component spectrum; (d) NC component spectrum. Note the presence of the 64 ppm resonance in (c); this is absent in spectrum 7c and suggests crystalline polymorphism.

apparent crystallinities deduced from the CP spectrum are distorted in part by the fact that during the 1 ms of cross polarization, proton polarization was decaying at different rates for the crystalline and the NC regions. One can, to a reasonable approximation, correct for this effect by measuring the initial rates of ^{13}C signal decay for different SL times prior to the fixed cross-polarization time. This correction is most sensitive to the shorter NC $T_{1\varrho}^{H}$, 3.4 ± 0.3 ms for both the RTA1 and the 85A samples. The longer $T_{1\varrho}^{H}$'s, associated with the crystalline regions, were, respectively, 30 ± 10 and 50 ± 10 ms. Using these values, crystallinities for the RTA1 and the 85A samples are, respectively, 0.27 ± 0.05 and 0.38 ± 0.05.

A more direct measure of crystallinity is obtained from the T_{1xz} and the T_{1xz}–spin-diffusion data.[24] Given that T_{1xz} decays, to a first approximation, occur in the absence of spin diffusion, the decays are simply the superposition of all of the individual proton decays. Also, since T_{1xz} values are sensitive to molecular motion,[23] the component with the longest decay in a semicrystalline solid is usually associated with the crystalline region; this is the case for PTEB. In order to isolate the T_{1xz} profile of the crystalline regions, we use the shape of the T_{1xz} decay associated with the T_{1xz}–spin-diffusion experiment for a t_{sd} chosen to be so short (30 μs) that negligible spin diffusion occurs prior to the T_{1xz} readout. Hence, the T_{1xz} readout in this case yields the T_{1xz} decay profile for the crystalline regions (T_{1xz} = 53 ± 8 and 101 ± 12 ms for the RTA1 and 85A samples, respectively), and this profile is used to assess its component strength in the overall T_{1xz} profile. Crystallinities deduced by this method are 0.25 ± 0.03 for the RTA1 sample and 0.35 ± 0.03 for the 85A sample. These numbers are in good agreement with those deduced from the ^{13}C spectra; they agree less well with the X-ray analysis of 0.40 ± 0.05 and 0.45 ± 0.05, respectively, although the trend is preserved. For purposes of estimating crystal thickness, we will use the mean values from all of these measurements, namely, 0.31 for the RTA1 sample and 0.39 for the 85A sample.

5. Long Spacing from T_{1xz}–Spin-Diffusion Measurements. The concept of the T_{1xz}–spin-diffusion experiment is described in the Experimental Section. In Figure 9 the data from this experiment are plotted against $t_{sd}^{1/2}$. The ordinate, ΔM, is given by

$$\Delta M = [\Delta M_c(t_{sd})/\Delta M_c(0)] \exp(t_{sd}/T_1^{H}) \qquad (1)$$

where $\Delta M_c(t_{sd})$ is the excess contribution to the total magnetization at t_{sd} arising from the crystalline regions;

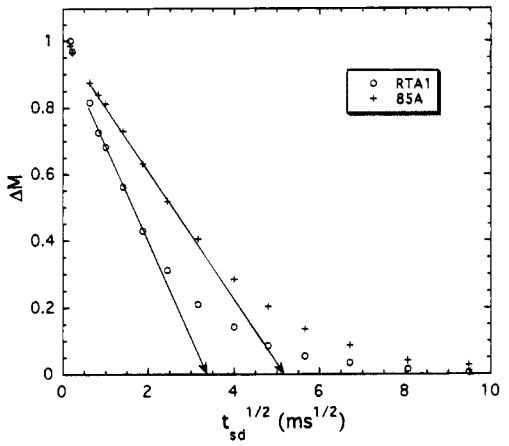

Figure 9. Decay of the excess "crystalline" magnetization, ΔM, toward internal spin equilibrium versus the square root of the spin diffusion time for the indicated samples. Overall repeat distances are calculated from the intercepts on the abscissa of the straight lines which capture the slopes in the vicinity of $t_{sd} = 1$ ms (the slope at earlier times may also contain a contribution from the dissipation of any initial gradients within monomers).

i.e., it is that contribution over and above that expected if the total magnetization arose from a uniform, "equilibrated", polarization per spin. The exponential term corrects for the longitudinal proton relaxation (T_1^H) processes which occur during this experiment. The range of ΔM is, by definition, $0 \leq \Delta M \leq 1$, where $\Delta M = 0$ represents the state of internal spin equilibrium.

Extraction of the long spacing from the data of Figure 9 is done[24,28] using the time intercepts of the indicated straight lines, which capture the early-time slopes. If we assume a lamellar morphology, which seems appropriate for a semicrystalline state with a smectic LC precursor, then the long period, L_{NMR}, is given by

$$L_{NMR} = 2(Dt_{sd}^*/\pi)^{1/2}/[f_c(1 - f_c)] \quad (2)$$

where t_{sd}^* is the square of the intercept, D is the spin diffusion constant, and f_c is the crystallinity. If, based on proton density, we estimate D[28,29] to be 500 nm^2/s and if the average f_c values from the previous section are used, then L_{NMR} values of 12.3 and 17.4 nm are obtained for the RTA1 and the 85A samples, respectively. Corresponding values deduced from the synchrotron data are 10.6 and 13.8 nm. The modest difference between these sets of values is, perhaps, partly rationalized by the uneven distribution of protons in PTEB, i.e., by the layering of proton-rich and proton-poor regions. These considerations would tend to reduce D (and L_{NMR}) from the value that was assumed. Nevertheless, these results allow us to make the following unambiguous conclusions: (a) There are no large (>100 nm) domains of pure LC order from which the synchrotron layer spacings arise. If there were, the curves in Figure 9 would not so closely approach 0. (b) The overall long spacing seen in the synchrotron data truly arises from the repeat distance between crystalline regions; there is no larger scale periodicity associated with crystal/NC variations.

6. Dynamic Differences between the LC and NC Regions. In this section we merely show that molecular mobility, as judged by various relaxation times, is comparable for the LC and the NC regions of the semicrystalline samples. By showing this comparability we are only offering a plausibility argument that intermolecular potentials are similar in the LC and NC regions, i.e., that mesogens and spacers are still segregated.

Table 2. Selected Relaxation Times[a] for Monitoring Changes in Molecular Mobility between the Liquid Crystalline State of the Quenched PTEB and the NC State of the Annealed PTEB Samples

			aliphatic		protonated aromatic
sample	region[b]	T_{1xz} (ms)	T_1^C (s)	$T_{1\varrho}^C$ (ms)	$T_{1\varrho}^C$ (ms)
Q	LC	2.3 ± 0.2	0.158 ± 0.015	2.7 ± 0.2	1.3 ± 0.1
RTA1	NC	3.6 ± 0.3			
85A	NC	3.8 ± 0.3	0.170 ± 0.015	3.7 ± 0.4[c]	0.9 ± 0.1

[a] Separation of the T_{1xz} components associated with the NC regions in the RTA1 and 85A samples was accomplished by subtracting from the T_{1xz} decay the contributions from the crystalline regions (see text) and assigning the difference curve to the NC component. The NC T_{1xz} was then assigned to that time at which this nonexponential difference decayed to e^{-1} of its initial value. The NC $T_{1\varrho}^C$ for the protonated aromatic carbons was measured directly by monitoring the change of aromatic wing intensity with ^{13}C spin locking time following cross polarization. The NC aliphatic T_1^C and $T_{1\varrho}^C$ measurements for the 85A sample were obtained from an analysis of the total aliphatic integrals along with the fact that, from line shape analysis, 55% of the total signal in the 85A sample arises from the NC region. Identifying the contributions from relaxation in the crystal was easy in the 85A sample since the ratio of crystal to NC relaxation times exceeded 10. Radio-frequency field strengths for the carbons and protons were, respectively, 69 and 66 kHz. [b] LC = liquid crystal; NC = noncrystalline. [c] This is the initial slope of the NC decay which, itself, is nonexponential, indicating the presence of NC components which relax on a longer time scale. The $T_{1\varrho}^C$ values for the crystalline components exceed 100 ms and thus are easily separable.

In Table 2 selected relaxation times assigned to the LC and NC regions are collected. The proton T_{1xz} and the ^{13}C rotating frame relaxation time, $T_{1\varrho}^C$, are sensitive to motions in the mid-kilohertz range while T_1^C is sensitive to motions in the MHz frequency range.[13] According to Table 2, T_1^C's are the same for the aliphatic carbons in the LC and NC regions. Methylene carbons with T_1^C's this short must exhibit large-amplitude motions with correlation times less than 10^{-7} s;[13] hence, in both the NC and LC regions, conformational interconversion is probably very facile. The slower motions probed by $T_{1\varrho}^C$ and T_{1xz} are also comparable; there is less than a factor of 2 difference between the LC and NC values for each relaxation time. The fact that the trend in $T_{1\varrho}^C$ values for the aliphatic and aromatic carbons is opposite is interesting but not particularly pertinent to this discussion. The mesogen and the spacer are expected to have very different mobilities. The spacer, as noted, has very fast motions. In contrast, the protonated aromatic carbons of the mesogen have a T_1^C in the Q sample of 1.2 ± 0.2 s (longer than their aliphatic counterparts) and a shorter $T_{1\varrho}^C$ than their aliphatic counterparts. Hence, there is more spectral density in the mid-kilohertz range for the aromatic versus the aliphatic carbons and more spectral density in the megahertz range for the aliphatic carbons. It is expected that the mesogen motion will be more sluggish than the motion of the spacer. Whether the trend in $T_{1\varrho}^C$ for the protonated aromatic carbons indicates that, relative to the LC state, crystallization disrupts some of the mesogen packing in the NC state (thereby allowing more motion) or whether motion of the mesogen in the LC state is on the fast side of the $T_{1\varrho}^C$ minimum (implying that crystallization slows down motion for the NC region) cannot be determined from these data.

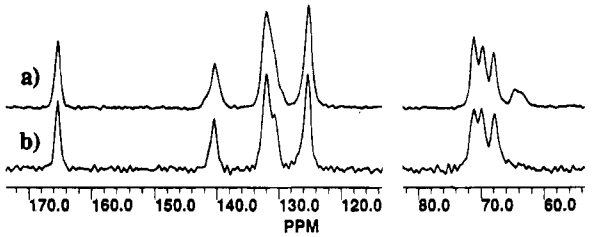

Figure 10. Comparison of the "crystal" component spectra: (a) 85A sample; (b) RTA1 sample.

7. Polymorphism. Most of our arguments about polymorphism relate to the ^{13}C spectra corresponding to the crystalline regions shown in Figures 7 and 8. These two spectra are collected in Figure 10 for purposes of easier comparison.

The simplest question regarding polymorphism is whether the crystalline state represented in the RTA1 and the 85A samples is the same. First, recall that the DSC traces for the RTA1 and the 85A samples showed considerable differences in the positions of the endotherms (Figure 2); the RTA2 sample had its largest endotherm at 64 °C while that of the 85A sample occurred at 108 °C. A second consideration regarding polymorphism relates to crystal thickness and whether the thin crystallites are capable of fully expressing their crystal habit in the spectra. If we use the average crystallinities previously deduced and the long spacings from the synchrotron data, then the thickness of the crystallites is only about 2 repeat units for the RTA1 sample and 3 repeat units for the 85A sample. When crystallites are this thin, one really cannot justify a detailed comparison of the spectra of the "crystalline regions". Moreover, one also does not know whether the crystal/NC interface occurs in the spacer or in the mesogen region, even though the flexibility of the spacer might favor its positioning at the point of transition from order to disorder.

In the light of the foregoing comments, we look at Figure 10 and note that there are only minor differences in these spectra, except for the resonance on the high-field side of the aliphatic region near 64 ppm (Figure 10a) associated with the 85A sample. Other minor differences in Figure 10a relative to Figure 10b are slightly different aliphatic multiplet splittings and small wings on the downfield side of the 140 ppm resonance and on the upfield side of the asymmetric resonance covering the 130−133 ppm range.

While we were initially tempted to argue that the above differences definitely indicated polymorphism for the crystallites in the RTA1 and 85A samples, we no longer insist on this because the finite crystal thickness may be the most important issue. It is conceivable that the difference in thickness is responsible for the difference in DSC melting points. It is also true that if we do not know where the crystal/NC interface is, the relative intensities in the "crystalline" spectra, associated with either the mesogenic or spacer carbons, will not necessarily correspond to their numbers in the PTEB repeat unit. That is especially true when the crystal thickness is only 2 repeat units. We note, however, that in the aliphatic region of spectrum 10b, the multiplet intensities correspond approximately to 6 carbons in the spacer (2 carbons assigned to each line); for the 85A sample, however, in Figure 10a, given that the 64 ppm feature is about 1/6th of the total aliphatic intensity, it is not obvious how one might assign the remaining 5 carbons in each spacer to the other multiplet intensities. One would expect these multiplet components to be in the ratio of small whole numbers, e.g. 2:2:1, but that is not true. Hence, this points to the following possibilities in the 85A sample: (a) polymorphism, (b) a unit cell with multiple, magnetically inequivalent repeat units, or (c) a problem associated with finite crystal thickness, as just outlined.

One final observation is pertinent regarding the 64 ppm peak in Figure 10a. The position of this peak compared to the high-resolution resonance positions (see Table 1) suggests that it arises from the C1 carbon (see Figure 1). Its unique chemical shift relative to all of the other aliphatic carbons in Figure 10 suggests that the conformation for these 64 ppm carbons is unique. Intrigued by this, we decided to monitor the intensity of this peak as a function of proton spin-locking time, prior to the 1 ms of cross polarization. If these unique carbons were near the crystal/NC interface, then, according to our computer modeling of spin diffusion during spin locking, the intensity of this 64 ppm feature should diminish, as spin lock time increases, relative to the other crystal resonances. The opposite occurred; i.e., there was about a 10% relative increase in intensity at locking times of 20 ms. Therefore, this resonance is definitely not associated with the interface; it is either associated with the interior of the crystalline regions in the 85A sample or there may even be polymorphism in the 85A sample, with the 64 ppm peak associated with the allomorph with the slightly longer $T_{1\varrho}^{H}$. (Recall that both the DSC and the synchrotron layer-line data offered some support for polymorphism in the 85A sample). On the other hand, if there is only one crystal form in PTEB and if all of the observed differences relate to finite crystal thickness, then the above observation may well mean that the conformation of the spacer in the crystal changes near the interface.

Conclusions

PTEB, which can be quenched into the smectic LC state, becomes semicrystalline (≈0.39 crystalline fraction) upon annealing for 12 days at 85 °C. Also, annealing for 33 months at ambient temperatures yields a 31%-crystalline sample, owing to a T_g of 20 °C. By ^{13}C NMR, the spectra of the crystalline fractions of these two semicrystalline samples are isolated. These two spectra, in the aromatic region, are very similar; however, in the aliphatic region there are significant differences which probably originate from conformational differences within the spacer. DSC data indicate significantly different crystalline melting points for the two samples. Polymorphism is one possible explanation for the differences in the NMR spectra as well as the DSC data. Small-angle synchrotron data, proton NMR spin diffusion data, and crystallinity values, combine to give a picture of relatively thin crystallites, about 3 repeat units thick in the 85A sample and about 2 units thick in the RTA1 sample. Thus, there is some question as to whether the crystallites are thick enough to express their undistorted crystalline habit in the ^{13}C spectra and whether the difference in the DSC melting points could possibly be attributed to a simple change in crystal thickness instead of polymorphism.

Synchrotron data taken in the region of the smectic layer spacing show that layer spacings persist in all samples, quenched or annealed. Yet there are definite changes in these layer spacings which accompany crystallization. In view of the thin nature of the crystallites, however, the relatively narrow width of

these synchrotron peaks suggests a periodicity which must encompass both the NC and the crystalline regions. Hence, there is probably a LC-like periodicity which remains in the NC regions, a view corroborated by an electron microscopy study[18] of another smectic LC system. Selected NMR relaxation measurements also bear out the notion that molecular mobility within the LC regions of quenched samples and the NC regions of semicrystalline samples is similar; i.e., corresponding relaxation times are different by no more than a factor of 2. These considerations, taken together, raise the question whether the tendency to preserve LC periodicity has any impact on the crystal unit cells which form and, in particular, on the conformation of the spacer. Such an influence may help to explain the differences in the spectra of the crystalline regions. Yet, we are skeptical of this latter point of view since the synchrotron results show that the layer spacing varies as much as 10% among these three samples with the greatest deviation from the LC spacing (and the smallest line width) seen in the RTA1 sample. This may reflect an alternate idea that the periodicity of the crystal which forms dictates the nearby layer spacing. The implications of this latter point of view are that layer spacings may be modified slightly without much cost in energy and that the crystal which forms under particular conditions need only possess a periodicity approximately like that of the original LC phase.

While the changes in layer spacing observed from the synchrotron data may suggest intriguing interpretations, one must be cautious. First, overall sample orientation could conceivably influence the position of this line. The LC smectic phase which forms in quenched PTEB possesses a smectic-C phase.[7] By examining an oriented sample, it was shown that there is an angle of about 23° between the chain direction and the normal to the smectic planes. The signature of the layer spacing in the WAXD photograph of this oriented sample was not an arc; moreover, this reflection does not have mirror symmetry about the meridional direction. In view of the foregoing, the position of the layer spacing we report may depend slightly on possible macroscopic orientation in our samples; we did not test for such orientation. Second, any variation in layer spacing observed may indicate an adjustment in the angle between the chain axis and the layer plane rather than a change in the average length of the repeat unit. Third, in view of the rather low levels of crystallinity which develop, even though the precursor state is a rather well organized LC state, it seems reasonable to conclude that the LC state does not represent a topologically simple, unentangled state. Rather, it is probably a topologically complicated state including many entanglements. Hence, the formation of crystallites, of necessity, concentrates entanglements in the NC regions. The impact of this infusion of topological "defects" on the layer spacing (or the chain tilt angle) is not known but may not be negligible.

Finally, in comparing the ^{13}C spectra of the respective crystalline regions in the RTA1 and the 85A samples, the most outstanding difference was the appearance, in the 85A sample, of an aliphatic-carbon resonance near 64 ppm, which probably arises from the C1 carbon. Its unique resonance position suggests a conformational difference, relative to other crystalline ester carbons. It was determined that these carbons, if they derived their unique resonance location from their spatial position relative to the crystal/NC interface, as opposed to their location in a separate crystalline allomorph, were near the interior of the crystal, rather than at the interface. Hence, in the 85A sample, if only one allomorph is present, then the conformation of the spacer in the interior of the crystal may be different from that nearer the interface. On the other hand, two allomorphs may be present, with different spacer conformations, in the 85A sample. The shape of the layer line in the synchrotron data tends to endorse this latter option.

We still consider polymorphism in PTEB to be a topic with several unanswered questions including just how many allomorphs there are and to what extent finite crystal thickness influences the NMR spectra or the DSC and scattering data.

Acknowledgment. Financial support from the Comisión Interministerial de Ciencia y Tecnología (Project No. MAT91-0380) and the Consejería de Educación de la Comunidad de Madrid is gratefully acknowledged. Also we acknowledge the support of NATO (Grant CRG 920094) in facilitating this interlaboratory collaboration. Dr. W. Bras and the Daresbury Laboratory (U.K.) are also thanked for their assistance in the synchrotron experiments.

References and Notes

(1) Ober, C. K.; Jin, J.; Fhou, Q.; Lenz, R. W. *Adv. Polym. Sci.* **1984**, *59*, 103.
(2) Varsney, S. K. *J. Macromol. Sci. Rev.* **1986**, *C26*, 551.
(3) Meurisse, P.; Noel, C.; Monnerie, L.; Fayolle, B. *Br. Polym. J.* **1981**, *13*, 55.
(4) Krigbaum, W. R.; Watanabe, J. *Polymer* **1983**, *24*, 1299.
(5) Watanabe, J.; Hayashi, M. *Macromolecules* **1988**, *21*, 278; **1989**, *22*, 4083.
(6) Pérez, E.; Bello, A.; Marugán, M. M.; Pereña, J. M. *Polym. Commun.* **1990**, *31*, 386.
(7) Pérez, E.; Riande, E.; Bello, A.; Benavente, R.; Pereña, J. M. *Macromolecules* **1992**, *25*, 605.
(8) Bello, A.; Riande, E.; Pérez, E.; Marugán, M. M.; Pereña, J. M. *Macromolecules* **1993**, *26*, 1072.
(9) Bello, A.; Pérez, E.; Marugán, M. M.; Pereña, J. M. *Macromolecules* **1990**, *23*, 905.
(10) Pérez, E.; Benavente, R.; Marugán, M. M.; Bello, A.; Pereña, J. M. *Polym. Bull.* **1991**, *25*, 413.
(11) Schaefer, J.; Stejskal, E. O.; Buchdahl, R. *Macromolecules* **1977**, *10*, 384.
(12) Earl, W. L.; VanderHart, D. L. *Macromolecules* **1979**, *12*, 762.
(13) Abragam, A. *The Principles of Nuclear Magnetism*; Oxford University Press: Oxford, 1961.
(14) Connor, T. M. *NMR* **1971**, *4*, 247.
(15) VanderHart, D. L.; Atalla, R. H. *ACS Symp. Ser.* **1987**, *340*, 88.
(16) Fyfe, C. A. *Solid State NMR for Chemists*, C.F.C. Press, Guelph, ON, 1983, Chapter 7.
(17) Pérez, E.; Marugán, M. M.; VanderHart, D. L. *Macromolecules* **1993**, *26*, 5852.
(18) Hudson, S. D.; Lovinger, A. J.; Gomez, M. A.; Lorente, J.; Marco, C.; Fatou, J. G. *Macromolecules* **1994**, *27*, 3357.
(19) Certain commercial companies are named in order to specify adequately the experimental procedure. This in no way implies endorsement or recommendation by the authors or their agencies.
(20) Vega, A. J.; Vaughan, R. W. *J. Chem. Phys.* **1978**, *68*, 1958.
(21) Mansfield, P.; Orchard, M. J.; Stalker, D. C.; Richards, K. H. B. *Phys. Rev.* **1973**, *B7*, 90.
(22) Rhim, W.-K.; Elleman, D. D.; Vaughan, R. W. *J. Chem. Phys.* **1973**, *59*, 3740.
(23) Mehring, M. Principles of High Resolution NMR in Solids, 2nd ed.; Springer-Verlag: Berlin, 1983, Chapter 8.
(24) Havens, J. R.; VanderHart, D. L. *Macromolecules* **1985**, *18*, 1663.
(25) Benavente, R.; Pereña, J. M.; Pérez, E.; Bello, A.; Lorenzo, V. *Polymer* **1994**, *35*, 3686.
(26) VanderHart, D. L.; Earl, W. L.; Garroway, A. N. *J. Magn. Reson.* **1981**, *44*, 361.
(27) VanderHart, D. L.; Pérez, E. *Macromolecules* **1986**, *19*, 1902.
(28) VanderHart, D. L.; Manley, R. St. J.; Barnes, J. D. *Macromolecules* **1994**, *27*, 2826.
(29) Douglass, D. C.; Jones, G. P. *J. Chem. Phys.* **1966**, *45*, 956.

MA946354Q